2018 7th IEEE International Conference on Biomedical
Robotics and Biomechatronics (Biorob)
Enschede, The Netherlands, August 26-29, 2018

A novel method for bilateral gait segmentation using a single thigh-mounted depth sensor and IMU

Blair H. Hu*, Student Member, IEEE, Nili E. Krausz*, Student Member, IEEE, and Levi J. Hargrove, Member, IEEE

Abstract— **Lower limb assistive devices have shown potential to restore mobility to millions of individuals with walking impairments; however, their success depends on whether they can be controlled safely, reliably, and intuitively with user-friendly sensors. To assist the user's walking patterns, many devices implement finite-state controllers which rely on accurate estimation of the current gait phase (e.g. stance, swing) of one or both legs. Bilateral gait segmentation is especially important for restoring natural interlimb coordination, which contributes to device safety and efficiency. Most existing techniques for gait segmentation use ground contact, device-embedded, or body-worn sensors with threshold or machine learning -based algorithms. They have been effective at identifying the state of the ipsilateral (i.e. sensor-side) leg but can become inconvenient for bilateral gait segmentation because they often require many sensors and are more sensitive to sensor placement. Therefore, we present a proof of concept for a novel approach to bilateral gait segmentation using a thigh-mounted inertial measurement unit (IMU) and depth sensor with the contralateral leg in its field of view. We extracted two features, ground and shank angle, from the depth data and developed a sensor fusion strategy to predict contralateral heel contact and ipsilateral toe off with accuracy approaching that of a setup with bilateral thigh and shank IMUs. By using computer vision to estimate the state of both legs, we introduce a new technique for bilateral gait segmentation which could make assistive devices more user-friendly, safe, and functional.**

I. Introduction

Recently, the field of wearable lower-limb assistive devices has expanded and there are now research and commercially available devices which can help restore locomotion. For example, powered prostheses have enabled amputees to seamlessly and intuitively transition between different locomotor activities including level ground, stairs, and ramps [1]–[3], while powered exoskeletons and orthoses have enabled individuals with paresis or paralysis to regain some functional independence by assisting transitions between sitting, standing, and level ground walking [4], [5]. Powered devices can actively change mechanical properties between different locomotor activities and can inject energy into the system (*e.g.* powered plantarflexion), which has potential to improve walking kinematics and overall mobility [6], [7]. However, users must demonstrate that they can control these powered devices safely, reliably, and intuitively with user-friendly sensors before these technologies will gain wider acceptance outside of the lab environment.

Gait phase-based methods, such as finite-state controllers, are most popular among numerous approaches for controlling wearable lower-limb assistive devices for different activities [8]. Finite-state controllers decompose gait into a series of distinct phases and parameterize the control laws based on the current state (*e.g.* stance, swing) and activity (*e.g.* standing, level walking). The first step to appropriately selecting and executing a control law within a finite-state paradigm, though, is state estimation (*i.e.* identifying the current gait phase).

Although most unilateral devices only estimate the state of the assisted side, bilateral state estimation is important for restoring safe and natural interlimb coordination. For instance, robust identification of the double support phase could help ensure a device does not become compliant before weight transfer, which could lead to buckling or a fall. Accurate detection of double support phase could also facilitate better synchronization of power delivery, making assistance such as powered plantarflexion more effective. Thus, incorporating bilateral state information into device function may also enable users to control their devices more intuitively and benefit more from the assistance they are capable of providing.

Many techniques have been developed for state estimation using body-worn and/or device-embedded sensors and a variety of detection algorithms [9]. For example, axial load and joint kinematics are used to transition between stance and swing states for a powered knee-ankle prosthesis [1]; however, load cells can be expensive and are not widespread outside of prosthetics. Foot switches and pressure sensitive insoles are also commonly used to derive a ground contact signal; however, they are sensitive to placement based on foot size and pressure distribution, limited by durability, and require a foot plate or shoe insert. Alternatively, electromyographic (EMG) signals have been used to detect up to 8 sub-phases of gait, but muscle signals are variable and instrumentation can be uncomfortable and inconvenient [9]. Finally, linear accelerometers, gyroscopes, and IMUs have been used for gait segmentation, sometimes in combination with ground contact sensors. Inertial sensors are small, cheap, and durable and can reliably estimate the state of the instrumented leg using algorithms based on peak detection and threshold crossings.

Though these existing techniques can accurately estimate the state of the instrumented leg, identifying the state of the uninstrumented leg poses some challenges. Thus, most unilateral assistive devices lack awareness of the state of the unassisted leg, which limits their ability to coordinate behavior between both legs. However, existing techniques for indirect sensing may be able to provide accurate and robust estimates

***B. H. Hu and N. E. Krausz contributed equally to this work.**

B. H. Hu was supported by USSOCOM Contract No. H92222-16-C-0111 and N. E. Krausz was supported by NIH T32 HD007418-23 Grant.

B. H. Hu, N. E. Krausz, and L. J. Hargrove are with the Center for Bionic Medicine at the Shirley Ryan AbilityLab (formerly RIC), Chicago, IL 60611 USA, and the Department of Biomedical Engineering, Northwestern University, Evanston, IL 60208 USA (corresponding: blairhu@u.northwestern.edu, nilikrausz2013@u.northwestern.edu).

L. J. Hargrove is also with the Department of Physical Medicine and Rehabilitation at Northwestern University, Evanston, IL 60208 USA.

978-1-5386-8183-1/18/$31.00 ©2018 IEEE

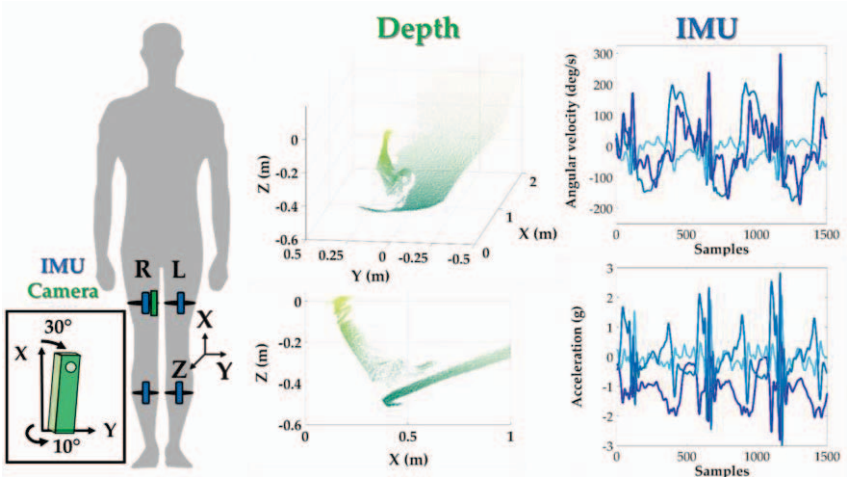

Figure 1. Sensor schematic. IMUs were placed bilaterally on the thigh and shank, and a single depth sensor was placed on the right thigh (internally rotated by ~10 degrees and tilted toward the ground by ~30 degrees). Isometric and side views of a single frame of raw depth data with the left (contralateral) foot visible are shown. The raw angular velocity and acceleration data from the right thigh IMU are also shown for part of a walking trial.

of the state of the uninstrumented leg while preserving user-friendly, unilateral sensorization.

Depth sensing is one such indirect sensing technique that may be useful for gait segmentation. Previously, a few studies have demonstrated the potential of using vision or depth sensing to detect changes in terrain to improve intent recognition [11]–[13]; however, to the best of our knowledge the use of a leg-mounted depth sensor for gait segmentation is unprecedented. With appropriate positioning and computer vision techniques, depth sensors could simultaneously provide high-confidence information about the environment, the contralateral leg, and the interaction between them.

In this paper, we present proof-of-concept for a novel approach using a single thigh-mounted depth sensor and IMU worn unilaterally to provide accurate and robust detection of bilateral gait events. We demonstrate that using depth sensor data to extract additional contextual information about the contralateral leg and the environment slightly improves bilateral gait segmentation. Our initial findings suggest that vision is a robust, non-redundant, and modular sensor modality that could improve the control of lower limb assistive devices.

II. Methods

A. Instrumentation and protocol

This study was carried out on one subject (male, 27 years old, 183 cm, 73 kg) after obtaining written informed consent as approved by the Northwestern University Institutional Review Board. The subject was instrumented with 6-DOF IMUs (tri-axial accelerometer and gyroscope) placed bilaterally on the thigh and shank and sampled at 500 Hz (MPU-9250; Invensense, San Jose, CA, USA). The sensors were attached to the subject with elastic straps and cohesive bandage. A 3D time-of-flight camera (Pico Flexx; Pmd Tech, Siegen, Germany [14]) was secured to the right thigh adjacent to the IMU with Velcro (Figure 1). The camera was positioned such that the left (contralateral) leg was visible during walking. The frame rate and resolution of the camera were set to 15 fps and 171x224 pixels, respectively.

Although ground contact sensors and embedded force platforms are commonly used to collect ground truth measurements of gait events, we chose an IMU-based segmentation approach instead so the subject could walk more freely and vary his path. Also, IMU-based segmentation approaches have been validated against more traditional techniques and are less sensitive to sensor placement [16].

The subject completed a total of 14 trials by performing two repetitions of each condition for three types of walking activities: (1) straight line walking at slow, normal, or fast speed for 10 meters, (2) straight or zig-zag walking at normal speed for 10 meters with obstacles in the path, and (3) straight line walking followed by a 90° right or left hand turn at normal speed for 15 meters. The wearable sensors were tethered and instrumentation setup took approximately 15 minutes.

B. IMU pre-processing

IMU signals were low-pass filtered (6th order, Butterworth) at 25 Hz. The estimated thigh and shank orientation angles relative to vertical were calculated using a complementary filter. To determine ground truth labels for the gait phase (stance or swing) of each leg, we applied an algorithm that searches for peaks and threshold crossings in the sagittal plane angular velocity of the shank segment [15]. Briefly, midswing events were identified as the maximum peaks, toe off events were identified as the minimum peaks just before midswing, and heel contact events were identified as the first zero-crossings after each midswing.

C. Depth sensor pre-processing

We recorded depth data frames as point clouds (171x224 pixels) using a Matlab library provided by the camera manufacturer [14]. We used the Matlab (R2017a) Computer Vision System Toolbox to convert point clouds into x, y, and z real-world dimensions. Point clouds were denoised to remove outliers above a threshold of 5 cm, and downsampled using a 1 cm grid filter for computational efficiency. The 3D point clouds and corresponding 2D projections were used as contextual information for segmenting the leg from the visual scene (Figure 2).

a) *Right leg:* Although the right leg was not in the camera's field of view, information about the movement of the environment (*i.e.* ground plane) can be used for gait segmentation. During stance, the leg rolls over the foot; thus, changes in leg orientation result in rotation of the environment relative to the camera reference frame. Therefore, the degree of rotation can be used to infer whether the right (ipsilateral) leg is in stance or swing phase (Figure 2a). First, we determined that the initial tilt of the environment due to camera positioning was approximately 30° (based on the ground orientation during a standing trial for which the subject remained stationary). To remove this initial rotation from the original point clouds, we applied an affine transform

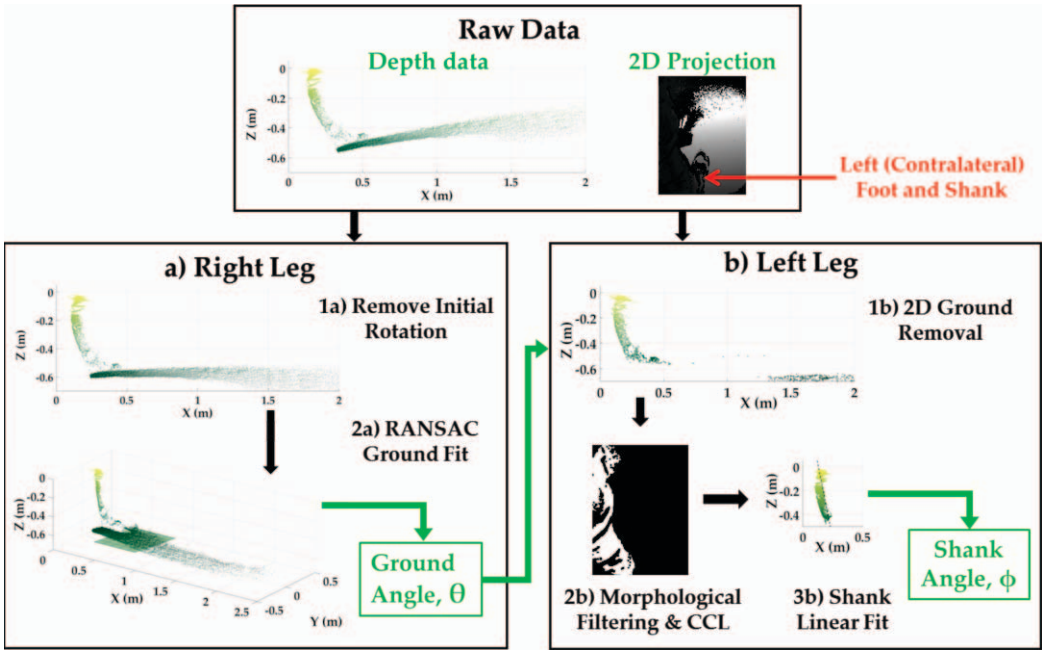

Figure 2. Depth sensor pre-processing flowchart. The raw depth data and 2D projection were used to produce an estimate of the ground angle (**θ**) and shank angle (**φ**) to estimate right toe off and left heel contact events, respectively.

based on an Euler angle rotation matrix. Next, we used RANSAC [17] to fit a plane to the points within a region of interest (ROI) directly in front of the user. The angle of this plane relative to horizontal was defined as the ground angle (**θ**) feature for detecting right toe off (RTO) events.

b) Left leg: When leading, the left leg was in the depth sensor's field of view, with the angle of the leg relative to the ground serving as a correlate of gait phase. We used the previously calculated ground angle, **θ**, to identify and remove points belonging to the ground plane from the point clouds and their 2D projections to simplify identification of the left leg. Next, to isolate connected regions in the ground-removed field of view we sequentially applied morphological thickening, closing, and hole filling to the binarized 2D projection. We performed connected component labeling (CCL) on remaining regions in the 2D projection, and regions with 500-10,000 pixels were labeled as the shank. We fit a border to the shank-labeled pixels and fit a line through the centroid of this shape using linear regression (Figure 2b). The angle of this line relative to vertical was defined as the shank angle (**φ**) feature for detecting left heel contact (LHC) events.

D. Gait event prediction

The depth and IMU data were temporally aligned by upsampling the depth data to match the IMU's sampling rate of 500 Hz. Next, the data were partitioned into 300 ms sliding windows (30 ms increment) to match current standards for online control of a powered leg prosthesis using intent recognition [1]. The ground truth (stance or swing) for each window was defined as the final label of the window. We used two independent methods (IMU or depth data only) to identify LHC and RTO events. Assuming a unilateral assistive device was worn on the right leg, LHC and RTO would represent the critical events spanning the double support phase of interest. Leave-one-out cross-validation was performed by training on the windows from all but one trial after aggregating trials from all walking activities. We assessed the accuracy of detecting LHC and RTO (within 200 ms of the corresponding ground truth) using the F_1 score and mean/standard deviation of the residuals between classifier predictions and the ground truth for all steps except for gait initiation and termination from all trials. Events detected more than 200 ms before/after the corresponding ground truth were considered outliers and excluded from the average.

IMU only: We compared different combinations of sensors including right thigh IMU only (R Thigh), right thigh and shank IMUs (R Thigh + Shank), and bilateral thigh and shank IMUs (R/L Thigh + Shank). Six features (mean, standard deviation, maximum, minimum, initial value, final value) were extracted from each window for each IMU channel (tri-axial accelerometer, tri-axial gyroscope, calculated orientation angle) for a total of 42 features per IMU sensor. These heuristic features were chosen because they are computationally efficient and are typically used in intent recognition for prosthesis control [1]. Features were normalized to have zero mean and unit variance and the

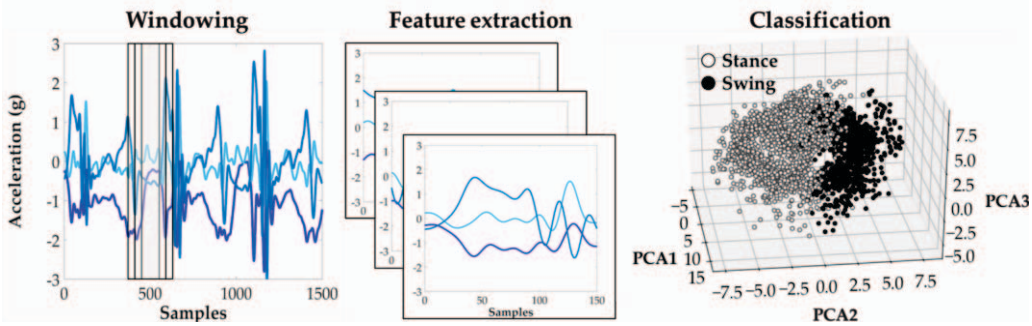

Figure 3. IMU estimate of gait event probabilities. IMU signals were partitioned into 300 ms sliding windows, from which statistical features were extracted. PCA was used to reduce the dimensionality to 25 and an LDA or SVM classifier was fit to predict stance or swing for each leg on a window-by-window basis.

dimensionality was reduced using principal components analysis (PCA) to 25 components, which accounted for more than 99 percent of the total variance (Figure 3). Preliminary results showed that the boundary between stance and swing in the feature space may be better represented by a nonlinear classifier. Therefore, we compared a linear discriminant analysis (LDA) classifier to a support vector machine (SVM) with Gaussian kernel for estimating probability of each class (stance or swing) to make predictions for each window.

Depth sensor only: The overall trajectories of the two depth-based features, rather than their magnitudes, were more consistently related to the timing of the predicted gait events. Therefore, unlike the IMU predictions, we used a template matching method to estimate the probability of detecting RTO and LHC from the ground and shank angles (Figure 4a). First, we created templates for RTO and LHC features by averaging the windows immediately preceding their respective ground truth gait events in the training data (Figure 4b). Next, we computed the element-wise product between each sliding window and the corresponding template and applied a binary mask outputting one for each point in the sliding window where the feature and template had matching signs and zero otherwise. Lastly, the probability of detecting a gait event in each window was estimated by averaging the output of the binary mask over the window length, yielding a value between 0 and 1 (Figure 4c). After tuning, a probability threshold of 0.55 was set to identify a range of candidate windows for detecting a gait event. Empirically, the range of possible RTO windows tended to end near the ground truth and the range of possible LHC windows tended to be centered near the ground truth (Figure 5). Therefore, RTO was predicted as the last window in the range and LHC was predicted as the window with highest probability (Figure 5).

Sensor fusion: We computed an equally weighted average of the probabilities of each event based on the IMU and the depth sensor separately. After tuning, a threshold of 0.55 was applied to the average probability to identify a range of possible windows for detecting gait events based on fusion of the right thigh IMU and depth sensor (Fused). Empirically, the range of possible LHC and RTO windows tended to begin near the corresponding ground truth; therefore, LHC and RTO were predicted as the first window in their respective range of windows (Figure 5).

III. Results

RTO and LHC predictions were made with LDA and SVM classifiers. The residuals for LHC predictions with SVM were -34 ± 96 ms (mean ± S.D.) with no outliers and -16 ± 63 ms with 2 outliers for R Thigh and Fused, respectively. The residuals for RTO predictions with SVM were 7 ± 30 ms with one outlier and 13 ± 60 ms with no outliers for R Thigh and Fused, respectively.

The LDA classifier outperformed SVM, so the results shown in Tables I and II are for LDA. Predictions for RTO were generally more accurate than for LHC when using right leg sensors only (in terms of mean, standard deviation, outliers, and F_1 scores). The average residuals were also mostly negative, meaning that events were predicted before the ground truth occurrence. Compared to predictions made using IMU sensors only, predictions with the depth sensor only had larger variability. There were also more outliers for LHC when using the depth sensor only, but outliers were reduced with sensor fusion. Unilateral sensor fusion slightly improved prediction accuracy compared to R Thigh, and approached the accuracy of R/L Thigh + Shank.

IV. Discussion

In this work we developed a novel approach to bilateral gait segmentation using a single IMU and depth sensor, both worn unilaterally on the right thigh. Our approach independently predicts left heel contact and right toe off events using data from the IMU only, depth sensor only, or both sensors together. The IMU-based predictions were made by either an LDA or SVM classifier trained with heuristic features. For the depth-based prediction, we extracted features from the

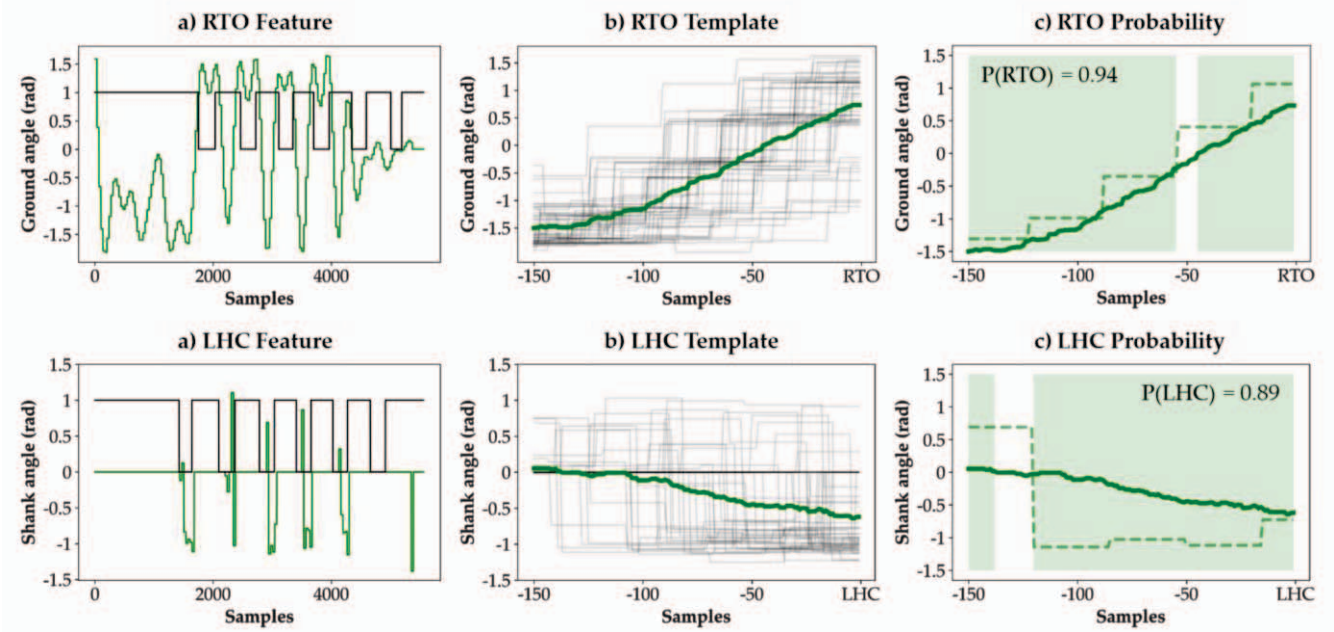

Figure 4. Depth sensor estimate of gait event probabilities. **(a)** Depth-based features for predicting right toe off (RTO) and left heel contact (LHC). The ground truth state (solid black) is either stance (1) or swing (0). **(b)** Templates (solid green) for depth-based features were calculated by averaging all 300 ms windows (solid gray) extracted just prior to ground truth RTO and LHC events in the training data. **(c)** The probability of detecting RTO and LHC for any given window was estimated by binarizing the element-wise product of the feature (dashed green) and its corresponding template (solid green). The probabilities of RTO and LHC are displayed (represented by the shaded proportion of the window).

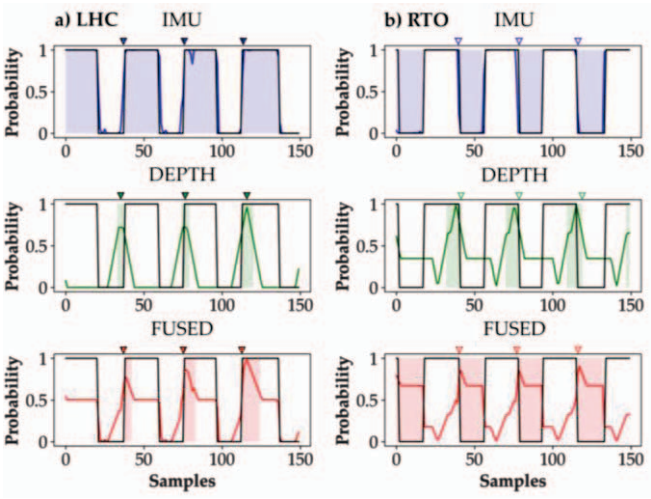

Figure 5. Gait event prediction. The solid colored traces represent the probabilities of detecting a) LHC and b) RTO. The shaded regions represent the range of possible windows for detecting a gait event using the R Thigh IMU only (IMU), depth sensor only (DEPTH), or both (FUSED). The tick marks represent the final predictions for LHC (filled) and RTO (empty).

environment and left leg, both in the field of view, and implemented a template matching algorithm to assign a probability of detecting each gait event. We fused the predictions using an equally weighted average of the IMU- and depth-based probabilities and assessed performance using the residuals and F_1 scores.

Our approach accurately detected both events (usually before the ground truth) for a variety of level ground walking tasks which included different speeds and paths. Without any additional adjustments, we did not notice any task-related changes in performance. As expected, we detected the ipsilateral (*i.e.* sensor side) toe off events more accurately than the contralateral heel contact events. Because the subject's interlimb coordination was intact, we also expected the prediction accuracy for left heel contact events using right leg IMUs to not deteriorate drastically. The classifiers trained with heuristic features from the IMU learned to associate right thigh kinematics with left leg state; however, we expect this association to weaken for subjects with gait impairments. Somewhat surprisingly, the depth sensor achieved low mean residuals for both gait events using only one depth-based feature for each prediction. Not surprisingly, using the depth sensor alone resulted in greater variability and more outliers for two main reasons.

First, we chose not to include the IMU into our estimate of the ground plane, which affected the segmentation of the contralateral foot. Because the outline of the foot was often sparse or absent after ground removal, we chose to estimate heel contact using shank angle. Shank angle served as a convenient proxy for detecting heel contact because it is related to foot rollover but it is only indirectly related to ground contact. The estimate of shank angle could have also been affected by movement of the sensor during walking and thresholding applied during image processing.

Second, the template matching procedure was sensitive to temporal misalignment and the binary masking operation based on the signs of the signals did not always adequately reflect the qualitative similarity between the sliding window and template. We also found that sensor fusion slightly improved prediction accuracy, approaching that of bilateral shank and thigh IMUs. Because predicting gait events using depth data makes no assumptions about interlimb coordination, we expected sensor fusion to improve prediction accuracy. We believe this is an important finding because it demonstrates that with sensor fusion, a unilateral setup can achieve similar accuracies to a bilateral setup.

TABLE I. ACCURACY OF LHC PREDICTIONS

	Number of steps = 57			
	Mean (ms)	***S.D. (ms)***	***Outliers***	***F_1***
R Thigh	-11	45	3	0.94
R Thigh + Shank	2	42	0	0.90
R/L Thigh + Shank	-6	34	0	0.97
Depth only	-14	85	13	0.87
R Thigh + Depth	-6	48	5	0.93

TABLE II. ACCURACY OF RTO PREDICTIONS

	Number of steps = 54			
	Mean (ms)	***S.D. (ms)***	***Outliers***	***F_1***
R Thigh	-6	41	0	0.97
R Thigh + Shank	2	35	0	0.98
R/L Thigh + Shank	-7	35	0	0.98
Depth only	-7	85	0	0.94
R Thigh + Depth	-5	39	0	0.92

Limitations and Future Work:

Although our proof of concept provided promising results, there are several limitations to this work. One limitation is that we only tested our algorithm on a limited number of level walking trials. We anticipate that some modifications, particularly to the ground and leg segmentation steps, may be necessary to adapt this algorithm to other activities such as ascending/descending stairs/ramps. We also excluded gait initiation and termination steps because their kinematics differ from steady state steps. Thus, a separate classifier may be required for accurately segmenting non-steady-state steps.

Our work is also limited by having only one able-bodied subject. In the future, we plan to assess the generalizability of our method to individuals with gait impairments, to a larger collection of walking data, and to testing and training on different subjects. We expect gait segmentation using unilateral IMU sensors to degrade for subjects with gait impairments or asymmetries, especially for identifying contralateral heel contact. Therefore, we expect the value of depth data for gait segmentation to be more evident when the assumption of intact interlimb coordination is violated.

We also propose several changes to the setup, protocol, and image processing. We did not use an independent sensor modality to acquire the ground truth for heel contact and toe off events for convenience. In the future, a force sensing resistor (FSR) could be used to provide an alternative estimate of the ground truth. We could also test our depth-based algorithm in different environments to determine its robustness to clutter, ground reflectance, and differently situated environments but our algorithm seemed to perform well even when obstacles were in the field of view.

Adding the pitch estimate from the thigh IMU to our calculation of the ground plane could have improved our predictions by preserving more of the foot during ground removal. In this work, we only tested one depth sensor configuration (frame rate, resolution, position), which may not have been optimized for spatiotemporal resolution and field of view for gait segmentation. Also, the positioning of the sensor on the thigh may not be ideal because it would not allow users to wear long pants or skirts. In the future, we will consider other positions that can capture both the environment and contralateral leg in the field of view. Additionally, we could use a single integrated sensor such as the Lenovo Phab 2 Pro [18] or Asus Zenfone AR [19], smartphones which integrate depth and inertial sensors. Additionally, in this work the depth sensing implementation was not optimized for timing, resulting in a computation time of 1.16 ± 0.56 s for extracting features from each point cloud. This is slower than desired, and in future work the computation time will be optimized and implemented in Python, rather than in Matlab.

We believe our approach to gait segmentation may be especially valuable for controlling powered assistive devices, because it would provide an additional safeguard to ensure the user is in double support phase before the device becomes compliant and transitions to swing phase. To validate the feasibility of our technique for powered prostheses, we will replicate our protocol with individuals walking with a powered knee-ankle prosthesis. Our approach may also be relevant to coordinating the behavior of two different unilateral devices which do not share sensors. Additionally, the features we used for gait segmentation (or others related to the contralateral leg position in space and its interaction with the environment) may also be improve prediction of the upcoming locomotor activity (*i.e.* intent recognition). For instance, the angle of the shank and height of the foot will likely differ between level ground walking, stair ascent and ramp ascent. Our overall goal will be to develop a system that performs gait segmentation and intent recognition in parallel. Finally, we will focus on online implementation of this system and integration with a powered prosthesis.

V. Conclusion

We developed a novel approach to bilateral gait segmentation based on a single IMU and depth sensor to predict right toe off and left heel contact events, which represent the beginning and end of a double support phase. The results of our proof of concept showed that predictions based on unilateral IMU and depth-based information approached the accuracy of using bilateral shank and thigh IMUs. By extending the use of depth data beyond environmental sensing to gait segmentation we provide an alternative strategy for sensing the state of both legs using wearable sensors, which could make assistive devices more user-friendly and improve their performance.

Acknowledgment

We thank Eric Earley for his help with the template matching algorithm and for the Whole Foods gift cards.

References

[1] A. M. Simon, K. A. Ingraham, J. A. Spanias, S. Member, A. J. Young, S. B. Finucane, E. G. Halsne, and L. J. Hargrove, "Delaying Ambulation Mode Transition Decisions Improves Accuracy of a Flexible Control System for Powered Knee-Ankle Prosthesis," *IEEE Trans. Neural Syst. Rehabil. Eng.*, vol. 25, no. 8, pp. 1164–1171, 2017.

[2] J. A. Spanias, A. M. Simon, S. B. Finucane, and E. J. Perreault, "Online adaptive neural control of a robotic lower limb prosthesis," *J. Neural Eng.*, vol. 15, 2018.

[3] H. Huang, F. Zhang, S. Member, L. J. Hargrove, Z. Dou, D. R. Rogers, K. B. Englehart, and S. Member, "Continuous Locomotion-Mode Identification for Prosthetic Legs Based on Neuromuscular – Mechanical Fusion," vol. 58, no. 10, pp. 2867–2875, 2011.

[4] H. A. Quintero, R. J. Farris, and M. Goldfarb, "A Method for the Autonomous Control of Lower Limb Exoskeletons for Persons with Paraplegia," *J. Med. Device.*, vol. 6, no. 4, p. 410031, 2012.

[5] A. J. Young and D. P. Ferris, "State of the Art and Future Directions for Lower Limb Robotic Exoskeletons," *IEEE Trans. Neural Syst. Rehabil. Eng.*, vol. 25, no. 2, pp. 171–182, 2017.

[6] B. E. Lawson, A. Huff, S. Members, and M. Goldfarb, "A Preliminary Investigation of Powered Prostheses for Improved Walking Biomechanics in Bilateral Transfemoral Amputees," *Int. Conf. IEEE EMBS*, pp. 4164–4167, 2012.

[7] K. A. Ingraham, N. P. Fey, A. M. Simon, and L. J. Hargrove, "Assessing the Relative Contributions of Active Ankle and Knee Assistance to the Walking Mechanics of Transfemoral Amputees Using a Powered Prosthesis," *PLoS One*, pp. 1–19, 2016.

[8] M. R. Tucker, J. Olivier, A. Pagel, H. Bleuler, M. Bouri, O. Lambercy, J. D. R. Millán, R. Riener, H. Vallery, and R. Gassert, "Control strategies for active lower extremity prosthetics and orthotics: a review.," *J. Neuroeng. Rehabil.*, vol. 12, no. 1, pp. 1–29, 2015.

[9] J. Taborri, E. Palermo, S. Rossi, and P. Cappa, "Gait Partitioning Methods : A Systematic Review," *Sensors*, vol. 16, no. 66, pp. 40–42, 2016.

[10] M. R. Tucker, J. Olivier, A. Pagel, H. Bleuler, M. Bouri, and O. Lambercy, "Control strategies for active lower extremity prosthetics and orthotics : a review Control strategies for active lower extremity prosthetics and orthotics : a review," *J. Neuroeng. Rehabil.*, vol. 12, no. 1, pp. 1–29, 2015.

[11] N. E. Krausz, T. Lenzi, and L. J. Hargrove, "Depth sensing for improved control of lower limb prostheses," *IEEE Trans. Biomed. Eng.*, vol. 62, no. 11, pp. 2576–2587, 2015.

[12] M. Liu, D. Wang, and H. Huang, "Development of an Environment-Aware Locomotion Mode Recognition System for Powered Lower Limb Prostheses," *IEEE Trans. Neural Syst. Rehabil. Eng.*, vol. 4320, no. c, pp. 1–1, 2015.

[13] Y. Massalin, S. Member, M. Abdrakhmanova, A. Varol, and S. Member, "User-Independent Intent Recognition for Lower-Limb Prostheses Using Depth Sensing," *IEEE Trans. Biomed. Eng.*, vol. 9294, no. c, 2017.

[14] PMD, "Camboard Pico Flexx." [Online]. Available: http://pmdtec.com/picofamily/.

[15] H. F. Maqbool, M. A. B. Husman, M. I. Awad, A. Abouhossein, P. Mehryar, and N. Iqbal, "Real - time gait event detection for lower limb amputees using a single wearable sensor *," *Int. Conf. IEEE EMBS*, pp. 5067–5070, 2016.

[16] J. M. Jasiewicz, J. H. J. Allum, J. W. Middleton, A. Barriskill, P. Condie, B. Purcell, R. Che, and T. Li, "Gait event detection using linear accelerometers or angular velocity transducers in able-bodied and spinal-cord injured individuals," *Gait Posture*, vol. 24, pp. 502–509, 2006.

[17] M. Fischler and R. Bolles, "Random sample consensus: a paradigm for model fitting with applications to image analysis and automated cartography," *Commun. ACM*, vol. 24, no. 6, 1981.

[18] Lenovo, "Phab 2 Pro," 2018. [Online]. Available: https://www3.lenovo.com/us/en/smart-devices/-lenovo-smartphones/phab-series/Lenovo-Phab-2-Pro/p/WMD00000220.

[19] Asus, "Zenfone AR," 2018. [Online]. Available: https://www.asus.com/us/Phone/ZenFone-AR-ZS571KL/.